Gait & Posture 112 (2024) 88–94

Contents lists available at ScienceDirect

Gait & Posture

journal homepage: www.elsevier.com/locate/gaitpost

# Investigation of intersegmental coordination patterns in human walking

Vaibhavsingh Varma, Mitja Trkov *

*Department of Mechanical Engineering, Rowan University, Glassboro, NJ 08028, USA*

ARTICLE INFO

*Keywords:*
Human locomotion
Intersegmental coordination
Planar covariation law
Limb elevation angles
Walking gait

ABSTRACT

*Background:* Intersegmental coordination between thigh, shank, and foot plays a crucial role in human gait, facilitating stable and efficient human walking. Limb elevation angles during the gait cycle form a planar manifold describes the by the planar covariation law, a recognized fundamental aspect of human locomotion.
*Research question:* How does the walking speed, age, BMI, and height, affect the size and orientation of the intersegmental coordination manifold and covariation plane?
*Methods:* This study introduces novel metrics for quantifying intersegmental coordination, including the mean radius of the manifold, rotation of the manifold about the origin, and the orientation of the plane with respect to the coordinate planes. A statistical investigation is conducted on a publicly available human walking dataset for subjects aged 19–67 years, walking at speeds between 0.18 and 2.3 m $s^{-1}$ to determine correlations of the proposed quantities. We used two sample t-test and ANOVA to find statistical significance of changes in the metrics with respect to gender and walking speed, respectively. Regression analysis was used to establish relationships between the introduced metrics and walking speed.
*Results:* High correlations are observed between walking speed and the computed metrics, highlighting the sensitivity of these metrics to gait characteristics. Conversely, negligible correlations are found for demographic parameters like age, body mass index (BMI), and height. Male and female groups exhibit no practically significant differences in any of the considered metrics. Additionally, metrics tend to increase in magnitude as walking speed increases.
*Significance:* This study contributes numerical metrics to characterize ISC of lower limbs with respect to walking speed along with regression models to estimate these metrics and related kinematic quantities. These findings hold significance for enhancing clinical gait analysis, generating optimal walking trajectories for assistive devices, prosthetics, or rehabilitation, aiming to replicate natural gaits and improve the functionality of biomechanical devices.

## 1. Introduction

Lower limb intersegmental coordination (ISC) is a critical aspect of human locomotion that involves precise control and synchronization of movements between the thigh, shank, and foot. This coordination is vital for maintaining balance, stability, and efficiency of locomotion. Planar Covariation Law (PCL) is a related principle and states that during walking and other forms of locomotion, the elevation angles of the lower limb segments (thigh, shank, and foot) covary along a specific plane. PCL was first described by Borghese et al. [1], and subsequent research has provided further insights into this phenomenon. Studies have confirmed the presence of planar covariation during normal walking, and in scenarios like walking on inclined surfaces, staircase stepping, and crouched or bent walking [2–4]. The gradual development of ISC among toddlers has also been reported [5,6]. Planar covariation has also been observed in gaits among animals including macaques, dogs, and quails [7–9]. All these observations suggest that the PCL is a fundamental principle that underlies various forms of human locomotion.

Researchers have used various quantities and metrics to evaluate the quality and nature of locomotion. General gait kinematic parameters like stride length, trunk kinematics, leg kinematics, phase differences between limbs, ground reactions, and knee moments have been observed to change with walking speed [10–14]. Fukuchi et al., in particular, have conducted a comprehensive review of over 500 subjects from various studies and reported that walking speed considerably affects both kinematic and kinetic parameters. In context of the ISC and PCL, Bianchi et al. [15] observed changes in orientation of the PCL plane

* Corresponding author.
*E-mail address:* trkov@rowan.edu (M. Trkov).

https://doi.org/10.1016/j.gaitpost.2024.05.010
Received 12 December 2023; Received in revised form 7 March 2024; Accepted 11 May 2024
Available online 13 May 2024

with walking speed using the direction cosine of the plane normal vector (vector normal/orthogonal to the PCL plane) with the thigh axis. Hicheur et al. [16] reported the changes of elevation angles for different walking speed groups and for backward walking. However, they also [16] argued that PCL may be an effect of high correlation between shank and foot movement rather than being a central constraint.

The thickness of the ISC manifold in the direction normal to the PCL plane has been used to note the differences between groups of young and old subjects having sedentary or active lifestyle [17]. Moderate standardized effect of age has been reported for ankle kinematics and small for hip and knee kinematics[18] whereas an effect on shank-foot coordination and increase of knee moment with age has been observed by Gueugnon et al. [19]. Age, gender, weight, and BMI have all been used as independent parameters to analyze dependence of different gait features [20], and also to develop multiple regression models for prediction of sagittal plane kinematics [21]. Correlation between a measure of intersegmental coordination which is – mean value of continuous relative phase (mCRP) – and age, weight, height, and walking speed has also been reported at different gait phases [14]. Wallard et al. [22] have shown that quantitative functional evaluation is useful in assessing differences in range of motion, intersegmental coordination, and work between groups of hip osteoarthritis patients, hemiparetic stroke patients, and healthy subjects. Although qualitative and quantitative observations of changes in kinematic quantities including joint angles, range of motion, step length, cadence and more have been presented in previous studies, detailed quantification of the changes in shape and size of ISC manifold and orientation of PCL plane has not been fully explored.

In this study, we investigated and characterized kinematic-based ISC manifolds in normal walking. We hypothesized that ISC manifolds varies with walking speed (speed) and might relate to age, height, gender, and BMI. Our specific aim was to quantify ISC manifolds through newly defined numerical metrics of mean radius of manifold (MRM), orientation of the ISC manifold, and orientation of the PCL plane itself. To characterize these quantities during walking, we conducted statistical analyses and derived regression models to estimate quantities based on the independent variables. The results and findings of our work contribute numerical metrics to assess ISC that can be used to enhance clinical gait analysis, and for the development of robust human-inspired gait controllers for assistive devices. The quantities could be incorporated within the controller to maintain or promote ISC and natural gait patterns generated by the assistive devices.

## 2. Methods

We examined a publicly accessible gait dataset with trials involving 50 subjects between 19 and 67 years old (24 women and 26 men, 37.0 ± 13.6 years, 1.74 ± 0.09 m, 71.0 ± 12.3 kg), walking at speeds ranging from 0.18 to 2.3 m $s^{-1}$ [23]. The dataset comprises 1143 clean walking trials categorized into five speed groups based on metronome-induced: S_0.1 (0.1–0.4 m $s^{-1}$), S_0.4 (0.4–0.8 m $s^{-1}$), S_0.8 (0.8–1.2 m $s^{-1}$) and self-selected: SS_1 (0.74–2.0 m $s^{-1}$), and SS_2 (1.2–2.3 m $s^{-1}$) speeds [23]. One full gait cycle in each trial was considered for all participants, and 5 trials were available at each speed group. Trial speeds were calculated using the average rate of change in the x-value of the TV10 marker [23] over one gait cycle. MATLAB 2022b (MathWorks, Inc., Natick, MA) was utilized with a custom script for data processing. Dataset was employed to observe changes in the nature of ISC manifold and PCL plane concerning speed, age, height, BMI, and gender, utilizing gait events provided as metadata to identify the gait cycle.

Sagittal plane elevation angles were computed from specific markers – hip and knee for thigh angle ($\theta_t$), knee and ankle for shank angle ($\theta_s$), and heel and toe for foot angle $\theta_f$ as shown in Fig. 1A. A normalization process, aligning with established practices [1,3,24], involved centering the ISC manifold around the coordinate origin by subtracting the mean, using $\theta_t$, $\theta_s$, and $\theta_f$ as axes which enables angle comparison across subjects.

Principal component analysis has been previously used to prove the planar relationship of the three limb elevation angles [3]. These principal components are derived using the eigenvalues and eigenvectors of the covariance matrix of the high dimensional data sample as per Eqs. (1) and (2) defined as

$$\det(\mathrm{cov}(X)-\lambda I) \quad = \quad 0 \tag{1}$$

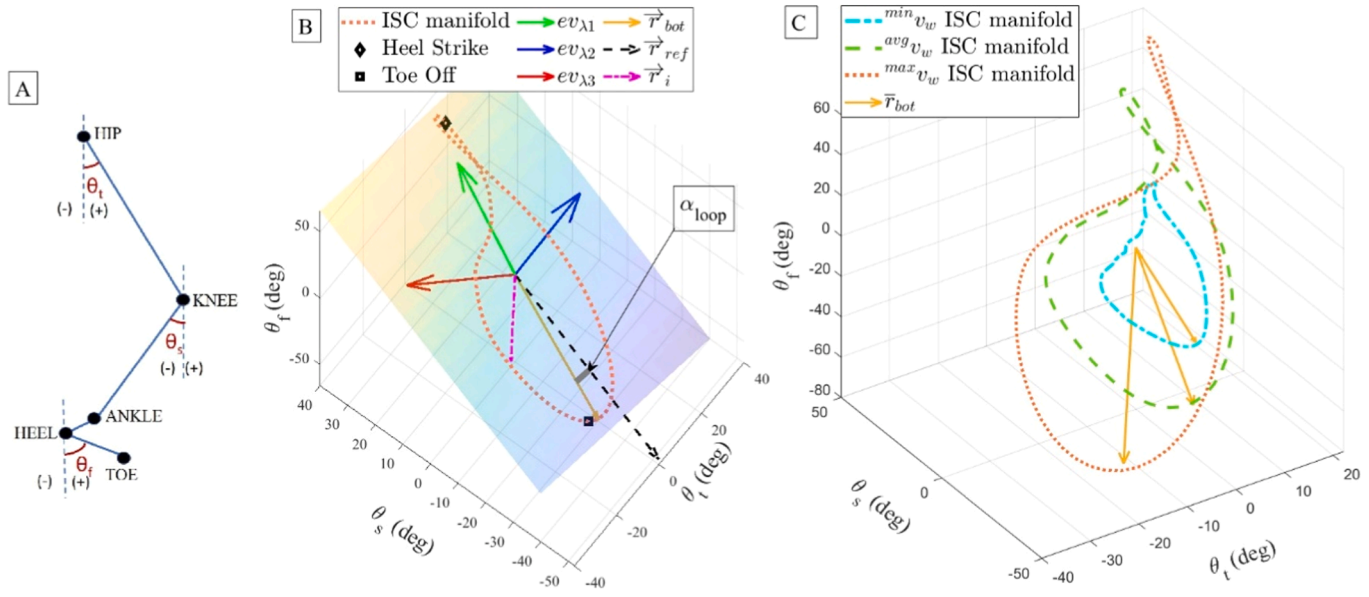


**Fig. 1.** (A) Repgn convention. $\theta_t$, $\theta_s$, and $\theta_f$ respectively represent thigh, shank, and foot elevation angles. HIP, KNEE, ANKLE, HEEL, and FOOT represent the markers placed on the subject corresponding to FTC, FLE, FAL, FCC, and FM2 marker names used by Schreiber and Moissenet [23]. (B) Representation of the ISC manifold and PCL plane with eigenvectors $\vec{ev}_{\lambda1}$, $\vec{ev}_{\lambda2}$ and $\vec{ev}_{\lambda3}$. $\vec{r}_i$ is the vector spanning from the origin to the *ith* data point on the ISC manifold. $\vec{r}_{bot}$ represents the vector from the origin to the lowest point on the ISC manifold in PCL plane. $\vec{r}_{ref}$ is a reference vector along the PCL plane and parallel to the foot-shank plane. $\alpha_{manifold}$ is the angle between $\vec{r}_{bot}$ and $\vec{r}_{ref}$ computed in the PCL plane. (C) Representative ISC manifolds for maximum, minimum, and average speed ($v_w$).

$$\mathrm{cov(X)}\quad \overrightarrow{\mathrm{ev}}_{\lambda i} = \quad \lambda_i \quad \overrightarrow{\mathrm{ev}}_{\lambda i} \tag{2}$$

where cov(X) is the 3 × 3 covariance matrix of the m × 3 dimensional elevation angle data, X. Size m represents the number of data samples, λ represents the eigenvalues. I is an 3 × 3 identity matrix. $\overrightarrow{\mathrm{ev}}_{\lambda i}$ are the eigenvectors corresponding to the ith eigenvalue $\lambda_i$. The eigenvectors define the PCL plane (see Fig. 2A). Here, the first two eigenvectors correspond to the two highest eigenvalues and lie along the PCL plane, while the third eigenvector is the plane normal vector.

Fig. 1B shows the representative ISC manifold with marked gait events and counterclockwise progression. ISC manifolds for minimum, maximum, and average speed from data set are shown in Fig. 1C. The magnitude of vector $\overrightarrow{r_i}$ represents the radius of manifold at the $i^{th}$ data point from the origin. The MRM metric, defined as $\Sigma|\overrightarrow{r_i}|/N$, has been introduced to quantify the variation of the size of ISC manifold, comprised of N data points. The rotation of the ISC manifold in the PCL plane has been quantified by the plane angle, $\alpha_{manifold}$. It is defined as the angle between a reference vector, $\overrightarrow{r}_{ref}$, that lies along the intersection of PCL plane with shank-foot plane, and the vector, $\overrightarrow{r}_{bot}$, pointing from the origin to the lowest point on the ISC manifold.

Ivanenko et al. [3] presented the changes of the direction cosine between PCL plane normal vector and thigh axis with respect to speed as a measure of orientation of the PCL plane. In this study, the change in 3D orientation of the PCL plane is quantified with the angles between the normal to the PCL plane and the coordinate planes. These are computed using Eqs. (3)–(5) defined as:

$$\tan(\Phi_{T-S}) = \frac{R}{\sqrt{P^2+Q^2}} \tag{3}$$

$$\tan(\Phi_{T-F}) = \frac{Q}{\sqrt{P^2+R^2}} \tag{4}$$

$$\tan(\Phi_{S-F}) = \frac{P}{\sqrt{Q^2+R^2}} \tag{5}$$

where $\Phi_{T\text{-}S}$, $\Phi_{T\text{-}F}$, and $\Phi_{S\text{-}F}$ are angles with respect to the thigh-shank, thigh-foot, and shank-foot planes, respectively. P, Q, and R are the components of the PCL plane normal vector, $\overrightarrow{\mathrm{ev}}_{\lambda min}$, along the thigh, shank, and foot axes respectively. The maximum and minimum limb angles of thigh ($^{max}\theta_t$, $^{min}\theta_t$), shank ($^{max}\theta_s$, $^{min}\theta_s$), and foot ($^{max}\theta_f$, $^{min}\theta_f$) have also been considered for analysis as these are directly related to the size and shape of the ISC manifold. Note that the 'max' and 'min' notations of quantities represent extreme values of limb elevation angles associated with the adopted convention (see Fig. 1A).

After computing all quantities, extreme outliers were identified and eliminated by assessing the dot product of each $\overrightarrow{\mathrm{ev}}_{\lambda min}$ with the mean of all plane normal vectors. Five outlier trials, with dot product values outside the three standard deviations range, were removed and attributed to unnatural gait particularly during the loading response phase induced by forced slow speeds (outlier speeds: 0.2794, 0.3147, 0.3422, 0.3256, and 0.3768 m $s^{-1}$). Subject age, height, BMI, and speed are independent variables for analyzing metric variations.

Pearson correlation matrix between independent variables and metrics provided an initial understanding of their relationships. Considering gender's potential role in ISC, metrics were grouped by female (522 trials) and male (616 trials). Two-sample t-tests and Cohen's d-statistic [25] determined significant and practical differences. Metrics were computed for all five speed groups. One-way ANOVA tested significant differences, supported by $\eta^2$ statistics for practical relevance (considering values 0.14 as large, 0.06 as medium, and 0.01 as small relevance) [25]. Despite S_0.1, S_0.4, and S_0.8 being metronome-induced, and SS_1 and SS_2 being self-selected speeds, all groups were considered for completeness. Regression analysis for metrics with respect to speed involved evaluating linear and quadratic curves. Selection was based on Bayesian information criterion (BIC) and root mean square error ($^{GM}$RMSE) between group means and predicted regression outputs at corresponding speed values, respecting data trends. The lower values of both BIC and $^{GM}$RMSE were used to select the optimal regression fit. $^{GM}$RMSEs were calculated between the group mean values for quantities in each speed group and the values predicted by the regression model at speeds corresponding to each group mean. If BIC and $^{GM}$RMSE values suggested different fits, BIC was given preference as a well-established metric in regression analysis.

## 3. Results

### 3.1. Correlation coefficients matrix

Pearson correlation coefficients for age, BMI, height, and speed with all the computed metrics are presented in Fig. 2. Speed has considerable correlation with all computed metrics except with $\Phi_{T-S}$. Age, BMI, and height do not present significant correlation with any of the quantities under consideration. This observation motivated further analysis of speed dependence. Although $\Phi_{T-S}$ has a negligible correlation with speed, it is still considered for further analyses for completeness. The relevant visualization for variations with respect to age, BMI, and height are presented in Supplementary material.

### 3.2. Evaluation of male and female groups

Fig. 3 consists of the bar plots showing the group means and ±1 standard deviation range for all computed metrics with corresponding statistic p-values and Cohen's d values. The p-values from the t-tests for MRM, $\alpha_{manifold}$, $\Phi_{T-S}$, $\Phi_{T-F}$, $^{min}\theta_t$, $^{max}\theta_s$, and $^{max}\theta_f$ suggest no significant differences between males and females. Even though p-values for $\Phi_{S-F}$, $\Phi_{T-F}$, $^{max}\theta_t$, $^{min}\theta_s$, and $^{min}\theta_f$ suggest that there are differences ($p < 0.01$) between male and female groups, Cohen's d value (< 0.5) suggests that the differences are practically insignificant.

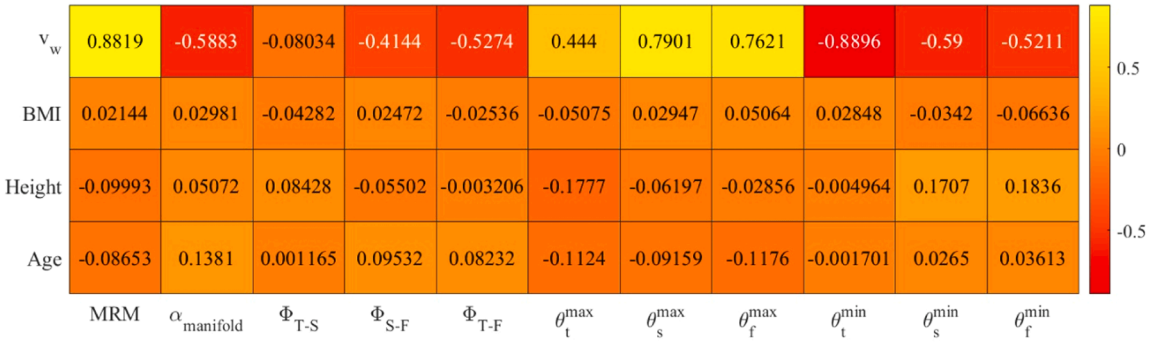


**Fig. 2.** Correlation coefficient matrix between independent variables and dependent computed quantities.

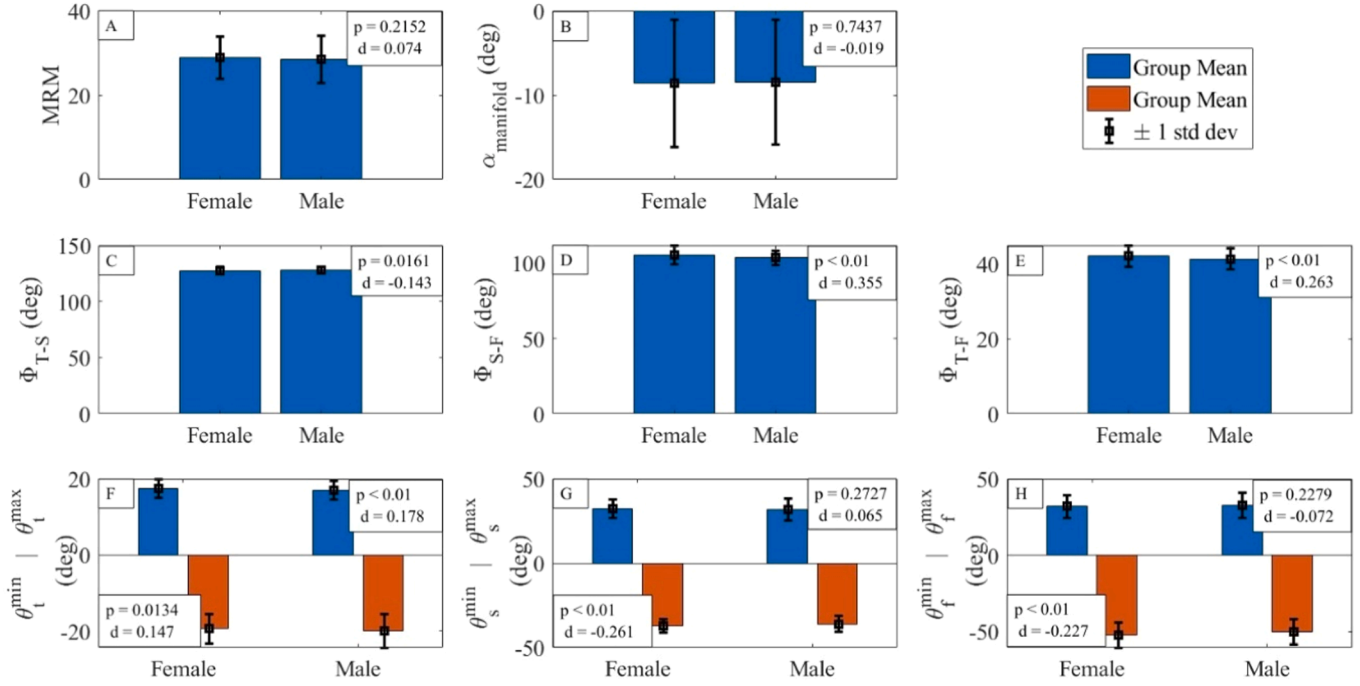


**Fig. 3.** Bar plots with ±1 standard deviation error bars representing means of all computed metrics MRM(A), $\alpha_{manifold}$ (B), $\Phi_{T-S}$ (C), $\Phi_{S-F}$ (D), $\Phi_{T-F}$ (E), the $^{max}\theta_t$ and $^{min}\theta_t$ (F), $^{max}\theta_s$ and $^{min}\theta_s$ (G), and $^{max}\theta_f$ and $^{min}\theta_f$ (H), grouped by male and female subjects. Textboxes represent statistic p-values and Cohen's d values.

### 3.3. Analysis of speed groups

One way ANOVA results for quantities divided into five walking speed groups are presented in Fig. 4. Despite low correlation between means of $\Phi_{T-S}$ and speed, low $\eta^2$ value (0.045) suggests no practically significant difference. All other quantities show practical importance ($\eta^2 > 0.14$) of changes with respect to speed.

### 3.4. Regression analysis with respect to speed

The results of regression analysis are presented in Table 1 and Fig. 5. Based on BIC and $^{GM}$RMSE values, $\Phi_{T-S}$, $^{min}\theta_t$, and $^{min}\theta_f$ dependencies of

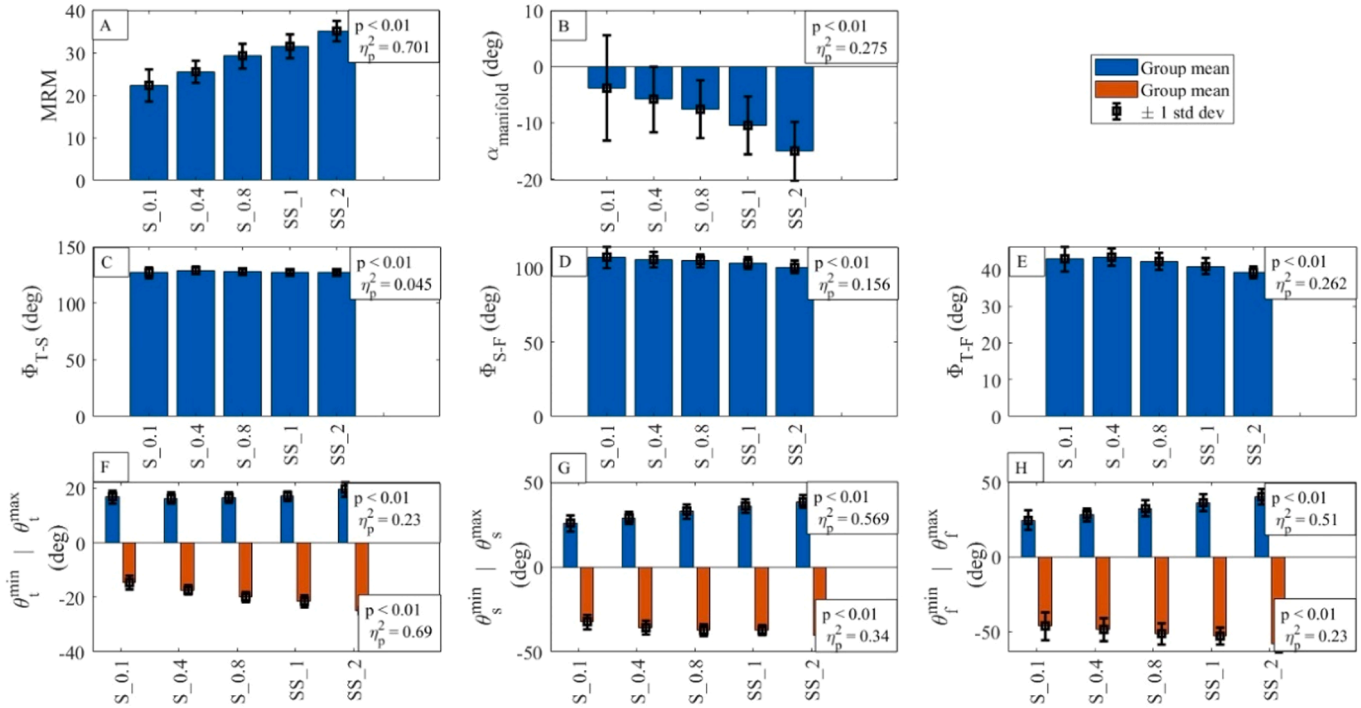


**Fig. 4.** Bar plots with ± 1 standard deviation error bars representing means of all computed metrics MRM(A), $\alpha_{manifold}$ (B), $\Phi_{T-S}$ (C), $\Phi_{S-F}$ (D), $\Phi_{T-F}$ (E), $^{max}\theta_t$ and $^{min}\theta_t$ (F), $^{max}\theta_s$ and $^{min}\theta_s$ (F), and $^{max}\theta_f$ and $^{min}\theta_f$ (F), grouped by walking speeds. The $\eta^2$ value for $\Phi_{S-F}$, shows practical significance as per the rule of thumb, however, it is still on the lower side due to the large within-group variances as compared to the magnitude of inter-group mean differences.

**Table 1**
Regression analysis for all computed metrics with respect to walking speed.

| | Linear Fit | | | | Quadratic Fit | | | | | |
|---|---|---|---|---|---|---|---|---|---|---|
| | RMSE | $R^2$ | $BIC_L$ | ${}^{GM}RMSE_L$ | RMSE | $R^2$ | $BIC_Q$ | ${}^{GM}RMSE_Q$ | $(BIC_L - BIC_Q)$ | $({}^{GM}RMSE_L - {}^{GM}RMSE_Q)$ |
| MRM | 2.530 | 0.778 | 5354.3 | 0.613 | 2.488 | 0.785 | 5322.1 | 0.705 | 32.2 | -0.092 |
| $\alpha_{manifold}$ | 6.039 | 0.346 | 7334.2 | 1.870 | 6.021 | 0.351 | 7333.5 | 1.264 | 0.7 | 0.607 |
| $\Phi_{T-S}$ | 3.255 | 0.006 | 5927.6 | 280.138 | 0.057 | 0.011 | 5929.7 | 280.177 | -1.9 | -0.039 |
| $\Phi_{S-F}$ | 5.163 | 0.172 | 6977.7 | 229.417 | 0.089 | 0.180 | 6973.1 | 229.509 | 4.6 | -0.076 |
| $\Phi_{T-F}$ | 2.441 | 0.278 | 5272.9 | 91.518 | 0.043 | 0.284 | 5270.6 | 91.556 | 2.3 | 0.042 |
| ${}^{max}\theta_t$ | 2.206 | 0.197 | 5042.8 | 1.712 | 2.042 | 0.313 | 4873 | 0.333 | 169.8 | 1.378 |
| ${}^{min}\theta_t$ | 1.897 | 0.791 | 4698.7 | 0.267 | 1.898 | 0.791 | 4705.4 | 0.275 | -6.7 | -0.008 |
| ${}^{max}\theta_s$ | 3.767 | 0.624 | 6260 | 1.526 | 3.709 | 0.636 | 6230.8 | 1.377 | 29.2 | 0.150 |
| ${}^{min}\theta_s$ | 3.623 | 0.348 | 6171.8 | 1.417 | 3.606 | 0.355 | 6167.1 | 1.347 | 4.7 | 0.070 |
| ${}^{max}\theta_f$ | 5.107 | 0.581 | 6952.7 | 1.567 | 5.068 | 0.588 | 6941.4 | 1.774 | 11.3 | -0.207 |
| ${}^{min}\theta_f$ | 7.048 | 0.272 | 7686.1 | 0.985 | 7.048 | 0.272 | 7692.1 | 1.342 | -6.0 | -0.358 |
| => | Metrics suggest linear fit is better | | | | | | | | | |
| => | Both metrics suggest different fit, but ($BIC_L$-$BIC_Q$) is given preference for selection | | | | | | | | | |
| => | Metrics suggest quadratic fit is better | | | | | | | | | |

speed were fitted with a linear model, while a quadratic model was used for all other quantities.

MRM increases with speed through a second order relationship and has a high positive coefficient of determination ($R^2 = 0.785$) (Fig. 5A). This indicates that the ranges of limb motions increase with speed. Fig. 5F–K show the changes in maximum and minimum elevation angles of each limb for different speed ranges. As speed increases from 0.18 m $s^{-1}$ to 2.3 m $s^{-1}$, ${}^{max}\theta_t$, ${}^{min}\theta_t$, ${}^{max}\theta_s$, ${}^{min}\theta_s$, ${}^{max}\theta_f$, and ${}^{min}\theta_f$ increase in magnitude by 8.9°, 16.8°, 19.0°, 10.3°, 24.3°, and 19.6°, respectively, along the regression line. The orientation of the ISC manifold in the PCL plane, $\alpha_{manifold}$, has an inverse second order relationship with speed as shown in Fig. 5B.

Fig. 5C–E show the variations of the PCL plane angles $\Phi_{T\text{-}S}$, $\Phi_{S-F}$, and $\Phi_{T\text{-}F}$ respectively. $\Phi_{S\text{-}F}$ and $\Phi_{T\text{-}F}$ show decreasing trend as speed increases, with $R^2 = 0.180$ and 0.284, respectively. The moderate values of correlation coefficients may be attributed to the large variance of the quantities for speed < 0.9 m $s^{-1}$. As shown in Fig. 5C, $\Phi_{T-S}$ has a linear relationship with a gradient of only − 0.55 and $R^2$ value of 0.0065 (lower than the threshold for practical significance)[25]. There was no improvement observed in curve fitting for any higher order relationships greater than the second order.

## 4. Discussion

We investigated the changes in ISC of lower limb elevation angles in relation to the walking speed. Novel metrics of MRM, which increases with increase in speed (Figs. 4A and 5A), and orientation angle $\alpha_{manifold}$ (Figs. 4B and 5B), which has a decreasing trend, indicate changes in ISC manifold, reflecting an increase in the range of motion. These results are in agreement with a previous study [12]. PCL plane orientation with respect to the thigh-shank plane, $\Phi_{T-S}$, does not show any particular trend (Fig. 5C). The trend for $\Phi_{S-F}$ observed in Fig. 5D suggests that PCL plane tends to become orthogonal to the foot-shank plane, as speed increases. $\Phi_{S-F}$ corresponds to the direction cosine used by others [3,10] and we observe similar trend. The PCL plane also tends to move closer to thigh-foot plane, observed through $\Phi_{T-F}$ in Fig. 5E, and it implies that the maximum and minimum foot elevation angles increase in magnitude. This observation was validated with the trends of ${}^{max}\theta_f$, and ${}^{min}\theta_f$ (Figs. 5H and 5K). Similarly, $\Phi_{S-F}$ trend corresponds to increase in magnitudes of ${}^{max}\theta_t$, and ${}^{min}\theta_t$ seen in Figs. 5F and 5I. Similar trends for increase in the range of motion with speed for healthy subjects have been presented for hip, knee, and ankle angles [22,26]. We quantified these trends by providing a regression model that best fits each of the metrics used in this study.

Statistical analyses on male and female groups revealed no gender-based differences in the metrics (Fig. 3). Age, height, and BMI also did not show much statistical effect on the computed ISC metrics (see Supplementary Material Figs. A1–A3). We observed small correlation values (< 0.13) for these metrics with respect to age and these correlations remain small even when evaluated separately for each speed group. The effect of walking speed on kinematics is more significant as compared to that of age [21,26]. Previous studies on ISC observed correlations with age for manifold thickness or ankle kinematics [17,19], however, their parameters were different and do not directly relate to our metrics. Although decreasing relationship has been reported for ankle range of motion with respect to age [19], our analysis did not reveal a significant trend for changes in ${}^{min}\theta_f$ and ${}^{max}\theta_f$ (which are closely relate to ankle range of motion) or any other metrics that we have computed (see Supplementary Material Fig. A1). Ogaya et al. [14] have shown that thigh-shank and shank-foot phase differences, are correlated with age and gait speed at different gait phases for elderly females. However, they suggest that the effect of gait speed prevails when controlling age, height, and weight, which is in agreement with findings of our study, where our parameters considered a complete gait cycle. It is also important to note that the dataset used in our study included subjects between 19 and 67 years, and therefore we were limited to considering young and middle-age population and not elderly population (> 75 years)[18].

Understanding the variations of MRM and elevation angle bounds with respect to walking speed is valuable for generating optimal trajectories for potential human-inspired controllers of assistive and prosthetic devices. MRM serves as a size measure of the ISC manifold and could aid in defining and controlling it. Future research may focus on creating optimal ISC patterns based on subject-specific biomechanical parameters, potentially improving controllers for robotic assistive devices during normal and perturbed gaits. For example, Aprigliano et al.

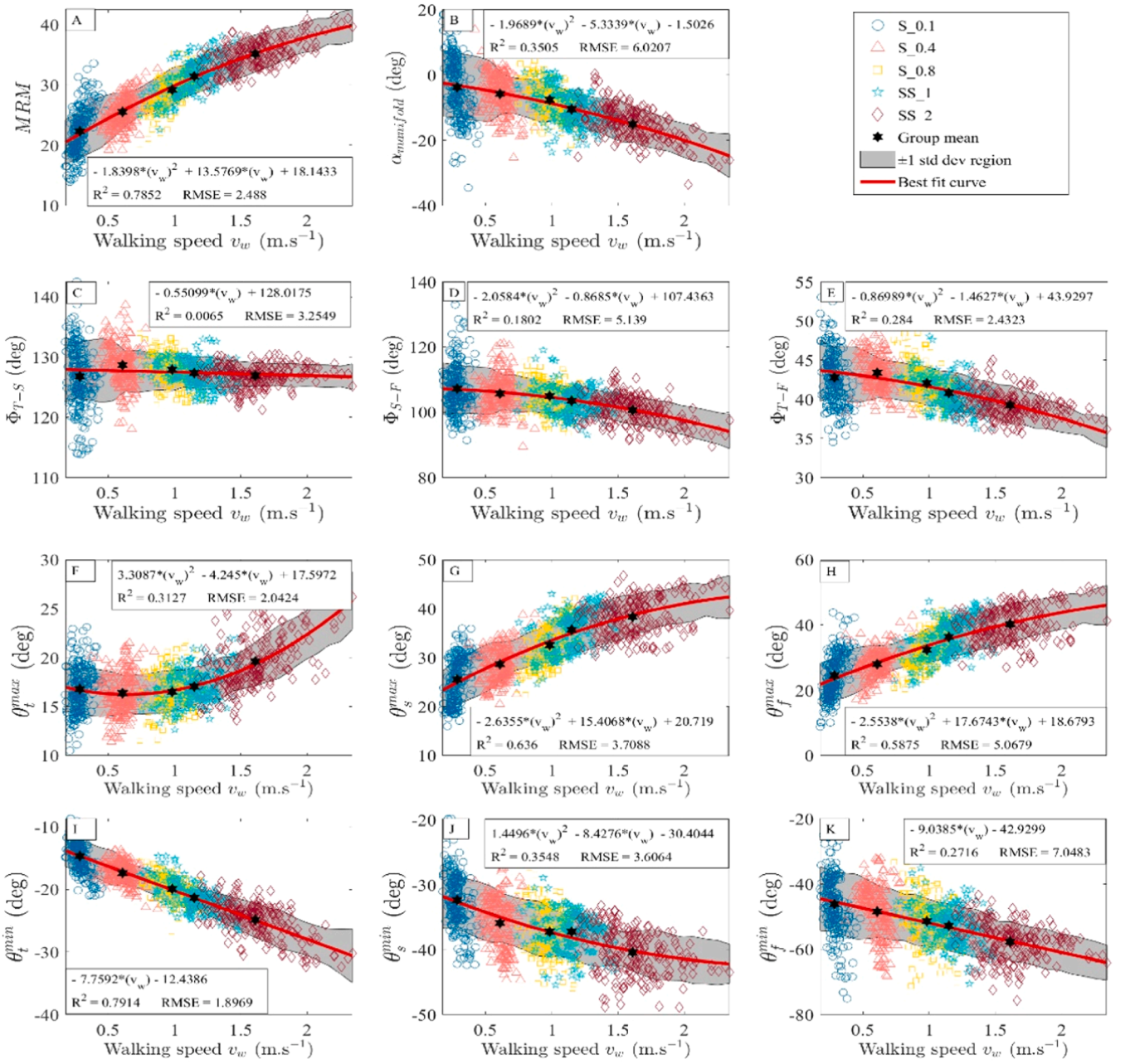


**Fig. 5.** Variations of MRM (A), $\alpha_{manifold}$ (B), $\Phi_{T-S}$ (C), $\Phi_{S-F}$ (D), $\Phi_{T-F}$ (E), ${}^{max}\theta_t$ (F), ${}^{min}\theta_t$ (G), ${}^{max}\theta_s$ (H), ${}^{min}\theta_s$ (I), ${}^{max}\theta_f$ (J), and ${}^{min}\theta_f$ (K) with respect to walking speed and corresponding regression curves with ± 1 standard deviation region and group means of quantities for each speed group.

[24] have explored the violation of PCL during slip perturbations. Further research on the nature of these violations could help in developing better fall prevention strategies. Extension of work done at the intersection of prosthetics and intersegmental coordination [27–29] is possible with the development of general ISC models along with the inclusion of kinetic parameters. ISC varies in pathological gait as compared to healthy gait [22] and quantitative assessment of pathological gait in terms of ISC with the use of metrics introduced in this study can be helpful in tuning assistive device controllers to adjust to subjects who exhibit such gait.

This study was limited to sagittal plane elevation angles for coordination, given their larger magnitudes than frontal and transverse planes. Future inclusion of frontal and transverse plane kinematics could provide additional insights. Large variances in parameters for slower walking speed groups influenced regression models. Despite slower speeds ($< 0.9$ m s$^{-1}$) being uncommon, as normal walking speeds lie in a range between 1.2 and 1.4 m s$^{-1}$ for adults of most ages [30], gait variations at such low speeds were included for completeness. Large variances may stem from subjects being asked to walk at unnaturally slow speeds. It has been reported that step time and double support time show high inter-subject variability at very slow walking speeds among healthy subjects [26] which can be considered a contributing factor to the large variances observed in our work as well.

In summary, we characterized ISC manifolds for walking gaits, revealing a proportional relationship between walking speed and MRM and orientation of ISC manifolds in the PCL plane. The quantifiable dependence of ISC and related kinematic parameters on walking speed, as demonstrated by models and trends, offers utility in predicting human walking behavior for assistive device controllers.

## CRediT authorship contribution statement

**Vaibhavsingh Varma:** Writing – review & editing, Writing – original draft, Visualization, Validation, Software, Methodology, Investigation, Formal analysis, Data curation. **Mitja Trkov:** Writing – review & editing, Supervision, Resources, Project administration, Methodology, Investigation, Funding acquisition, Formal analysis, Conceptualization.

## Declaration of Competing Interest

The authors declare that they have no known competing financial interests or personal relationships that could have appeared to influence the work reported in this paper.

## Acknowledgement

This material is based upon work partially supported by the National Science Foundation under Grant no. 2301816.

### *Declarations of interest*

None.

### *Conflict of Interest Statement*

The authors declare no conflicts of interest.

## Appendix A. Supporting information

Supplementary data associated with this article can be found in the online version at doi:10.1016/j.gaitpost.2024.05.010.

## References

[1] N.A. Borghese, L. Bianchi, F. Lacquaniti, Kinematic determinants of human locomotion, J. Physiol. 494 (1996) 863–879.
[2] R. Grasso, M. Zago, F. Lacquaniti, Interactions between posture and locomotion: motor patterns in humans walking with bent posture versus erect posture, J. Neurophysiol. 83 (2000) 288–300, https://doi.org/10.1152/jn.2000.83.1.288.
[3] Y.P. Ivanenko, A. d'Avella, R.E. Poppele, F. Lacquaniti, On the origin of planar covariation of elevation angles during human locomotion, J. Neurophysiol. 99 (2008) 1890–1898, https://doi.org/10.1152/jn.01308.2007.
[4] J.W. Noble, S.D. Prentice, Intersegmental coordination while walking up inclined surfaces: age and ramp angle effects, Exp. Brain Res. 189 (2008) 249–255.
[5] G. Cheron, E. Bouillot, B. Dan, A. Bengoetxea, J.P. Draye, F. Lacquaniti, Development of a kinematic coordination pattern in toddler locomotion: planar covariation, Exp. Brain Res. 137 (2001) 455–466, https://doi.org/10.1007/s002210000663.
[6] Y.P. Ivanenko, N. Dominici, G. Cappellini, F. Lacquaniti, Kinematics in newly walking toddlers does not depend upon postural stability, J. Neurophysiol. 94 (2005) 754–763, https://doi.org/10.1152/jn.00088.2005.
[7] G. Catavitello, Y.P. Ivanenko, F. Lacquaniti, Planar covariation of hindlimb and forelimb elevation angles during terrestrial and aquatic locomotion of dogs, vol. 10, n.d., e0133936. ⟨https://doi.org/10.1371/journal.pone.0133936⟩.
[8] N. Ogihara, T. Kikuchi, Y. Ishiguro, H. Makishima, M. Nakatsukasa, Planar covariation of limb elevation angles during bipedal walking in the Japanese macaque, vol. 9, 2012, pp. 2181–90. ⟨https://doi.org/10.1098/rsif.2012.0026⟩.
[9] N. Ogihara, T. Oku, E. Andrada, R. Blickhan, J.A. Nyakatura, M.S. Fischer, Planar covariation of limb elevation angles during bipedal locomotion in common quails (*Coturnix coturnix*), n.d. ⟨https://doi.org/10.1242/jeb.109355⟩.
[10] A.H. DeWolf, G.M. Meurisse, B. Schepens, P.A. Willems, Effect of walking speed on the intersegmental coordination of lower-limb segments in elderly adults, vol. 70, 2019, pp. 156–61. ⟨https://doi.org/10.1016/j.gaitpost.2019.03.001⟩.
[11] C.A. Fukuchi, R.K. Fukuchi, M. Duarte, Effects of walking speed on gait biomechanics in healthy participants: a systematic review and meta-analysis, Syst. Rev. 8 (2019) 1–11, https://api.semanticscholar.org/CorpusID:195758417.
[12] H.G. Kang, J.B. Dingwell, Separating the effects of age and walking speed on gait variability, Gait Posture 27 (2008) 572–577, https://doi.org/10.1016/j.gaitpost.2007.07.009.
[13] C. Kirtley, M.W. Whittle, R.J. Jefferson, Influence of walking speed on gait parameters, J. Biomed. Eng. 7 (1985) 282–288, https://doi.org/10.1016/0141-5425(85)90055-X.
[14] S. Ogaya, A. Iwata, Y. Higuchi, S. Fuchioka, The association between intersegmental coordination in the lower limb and gait speed in elderly females, Gait Posture 48 (2016) 1–5, https://doi.org/10.1016/j.gaitpost.2016.04.018.
[15] L. Bianchi, D. Angelini, F. Lacquaniti, Individual characteristics of human walking mechanics, Pflügers Arch. 436 (1998) 343–356.
[16] H. Hicheur, A.V. Terekhov, A. Berthoz, Intersegmental coordination during human locomotion: does planar covariation of elevation angles reflect central constraints? J. Neurophysiol. 96 (2006) 1406–1419, https://doi.org/10.1152/jn.00289.2006.
[17] D. Abe, K. Motoyama, T. Tashiro, A. Saito, M. Horiuchi, Effects of exercise habituation and aging on the intersegmental coordination of lower limbs during walking with sinusoidal speed change, J. Physiol. Anthr. 41 (2022) 1–9, https://doi.org/10.1186/s40101-022-00298-w.
[18] K.A. Boyer, R.T. Johnson, J.J. Banks, C. Jewell, J.F. Hafer, Systematic review and meta-analysis of gait mechanics in young and older adults, Exp. Gerontol. 95 (2017) 63–70, https://doi.org/10.1016/j.exger.2017.05.005.
[19] M. Gueugnon, P.J. Stapley, A. Gouteron, C. Lecland, C. Morisset, J.-M. Casillas, et al., Age-related adaptations of lower limb intersegmental coordination during walking, Front. Bioeng. Biotechnol. 7 (2019) 173.
[20] E.F. Chehab, T.P. Andriacchi, J. Favre, Speed, age, sex, and body mass index provide a rigorous basis for comparing the kinematic and kinetic profiles of the lower extremity during walking, J. Biomech. 58 (2017) 11–20, https://doi.org/10.1016/j.jbiomech.2017.04.014.
[21] F. Moissenet, F. Leboeuf, S. Armand, Lower limb sagittal gait kinematics can be predicted based on walking speed, gender, age and BMI, Sci. Rep. 9 (2019) 9510, https://doi.org/10.1038/s41598-019-45397-4.
[22] L. Wallard, S. Boulet, O. Cornu, J.-E. Dubuc, P. Mahaudens, D. Postlethwaite, et al., Intersegmental kinematics coordination in unilateral peripheral and central origin: effect on gait mechanism? Gait Posture 62 (2018) 124–131, https://doi.org/10.1016/j.gaitpost.2018.03.014.
[23] C. Schreiber, F. Moissenet, A multimodal dataset of human gait at different walking speeds established on injury-free adult participants, Sci. Data 6 (2019) 111. https://doi.org/10.1038/s41597-019-0124-4.
[24] F. Aprigliano, V. Monaco, S. Micera, External sensory-motor cues while managing unexpected slippages can violate the planar covariation law, J. Biomech. 85 (2019) 193–197.
[25] P.D. Ellis, Effect sizes and the interpretation of results, in: The Essential Guide to Effect Sizes: Statistical Power, Meta Analysis and the Interpretation of Research Results, Cambridge University Press, 2010, pp. 3–44.
[26] A.R. Wu, C.S. Simpson, E.H.F. van Asseldonk, H. van der Kooij, A.J. Ijspeert, Mechanics of very slow human walking, Sci. Rep. 9 (2019) 18079, https://doi.org/10.1038/s41598-019-54271-2.
[27] N. Krausz, T. Flash, Asymmetric changes in intersegmental covariation across ambulation levels and prosthetic devices for transfemoral amputee gait, in: Proceedings of the 2023 11th International IEEE/EMBS Conference on Neural Engineering (NER), 2023, pp. 1–6. ⟨https://doi.org/10.1109/ner52421.2023.10123729⟩.
[28] S. Ranaldi, C. De Marchis, M. Serrao, A. Ranavolo, F. Draicchio, F. Lacquaniti, et al., Modular control of kinematics in prosthetic gait: low-dimensional description based on the planar covariation law, in: A., M.-K.S., M.D. Jarm Tomaz, Cvetkoska (Eds.), 8th European Medical and Biological Engineering Conference, Springer International Publishing, Cham, 2021, pp. 833–9.
[29] S. Ranaldi, C. De Marchis, M. Serrao, A. Ranavolo, F. Draicchio, F. Lacquaniti, et al., Characterization of prosthetic knees through a low-dimensional description of gait kinematics, J. Neuroeng. Rehabil. 20 (2023) 1–11, https://doi.org/10.1186/s12984-023-01160-5.
[30] O. Mohamed, H. Appling, 5 – clinical assessment of gait, in: K.K. Chui, M. "Millee" Jorge, S.-C. Yen, M.M. Lusardi (Eds.), Orthotics and Prosthetics in Rehabilitation, Fourth Edition, Elsevier, St. Louis (MO), 2020, pp. 102–143, https://doi.org/10.1016/B978-0-323-60913-5.00005-2.